Chalcogenide Letters Vol. 19, No. 9, September 2022, p. 627 - 635

Optical damage and the third-order nonlinearity in GeGaS glasses

T. X. Wei, Z. Zhang, Z. Yang, Y. Sheng*, R. P. Wang
The Research Institute of Advanced Technologies, Ningbo University, Ningbo 315211, China

We have measured optical properties of $Ge_xGa_4S_{96-x}$ (x=22.5, 27, 30, 33.3 and 36) glasses including optical bandgap E_g, hardness, linear and nonlinear refractive index and laser damage threshold. We found that, both E_g and laser damage threshold exhibit maximum values in $Ge_{30}Ga_4S_{66}$ glass, linear refractive index increases with increasing Ge content, but nonlinear refractive index has a minimum in $Ge_{30}Ga_4S_{66}$, and their correlation can be well described by the Miller's rule. We conclude that, $Ge_{30}Ga_4S_{66}$ glass with chemically stoichiometric composition might be ideal for the chalcogenide-based optical amplifiers since it has reasonable optical nonlinearity, and high figure of merit (FOM) and laser damage threshold.

(Received June 10, 2022; Accepted September 21, 2022)

Keywords: Nonlinearity, Laser damage, Chalcogenide glasses

1. Introduction

Rare earth ions (REI)-doped chalcogenide glasses can be used in various passive and active photonics devices like planar waveguide-based sensing and laser emission in mid-infrared, because of their high linear and nonlinear refractive index, broad transmission range up to 25 μm, and low phonon energy [1-3]. For example, large optical nonlinearity can effectively enhance the interaction between the glasses and the molecules absorbed on the surface of the glasses and thus increase the efficiency of the sensor[4,5]. The radiative emission quantum efficiency of rare-earth ions can be increased by lower phonon energy in the host glasses, making it possible to use REI-doped chalcogenide glasses for the applications as optical amplifier or lasing in the midinfrared[6,7]. For these reasons, extensive investigation on REI-doped chalcogenide glasses have been reported to develop optical amplifiers or lasers working at the mid-infrared [1-8].

However, it was found that, REIs are hard to be directly doped into chalcogenide glasses since the REI ions are prone to form clusters in the glasses, leading to the quenching of the photoluminescence[6,7]. For example, typical As_2S_3 glasses only can host 0.1% mol Er. It was found that, Ga can be well dissolved in the glasses, and adding metallic Ga into glass matrix can reduce the number of the REI clusters via the formation of Ga-REI bonds. Compositional ratio of Ga to REI around 10:1 is preferential to dissolve the REIs into the host glasses and the maximum REI doping content is around 1% mol [6,7].

While typical Ge-Ga-S and Ge-Ga-Se glasses have been well used as hosts for REI doping, there are two essential issues that have not been systematically investigated yet. First, the third order optical nonlinearity of the glass is correlated with its chemical composition. Several different n_2 values have been reported in the previous literatures. For example, Dong et.al. reported a value of 4.13×10^{-15} cm^2/W in $(GeS_2)_{90}(Ga_2S_3)_{10}$ glass at 820 nm[12], Guo et.al reported a value of 4.46×10^{-14} cm^2/W in $(GeS_2)_{80}(Ga_2S_3)_{20}$ at 800 nm [13] which is one order of magnitude larger than the former one, although the glass composition is slightly different. More recently, a n_2 value of 1.7×10^{-14} cm^2/W was reported at 1550 nm for $Ge_{25}Ga_{10}S_{65}$ glass [14]. While these n_2 data were measured in random composition, there is no systematic investigations on how the optical nonlinearity and two-photon absorption coefficient evolves with the glass composition, but this is important to find out the best glass used in optical devices. Second, for practical applications,

* Corresponding authors: shengyan@nbu.edu.cn
https://doi.org/10.15251/CL.2022.199.627

chalcogenide-based optical devices are usually pumped by various ultrashort pulsed lasers. For example, femtosecond laser pulses with a wavelength near the zero dispersion wavelength of the devices are usually used to pump chalcogenide-based fibres or waveguides for supercontinuum generation [9-11]. Thus, it is important to make sure that, the pumping power should be less than damage threshold of the glass used in any optical devices. However, there is no related data on the laser damage of GeGaS glasses.

In the present paper, we prepared $Ge_xGa_4S_{96-x}$ glasses with x from 22.5 to 36, and measured various physical parameters like glass transition temperature (T_g), density, hardness, and linear and nonlinear optical parameters at 1.5 μm and the laser damage thresholds using 800 nm fs laser. From the data, we proposed that chemically stoichiometric GeGaS glass might be the best as the host glass for REI doping for the active applications in optical amplifiers or lasers.

2. Experiments

The glasses were synthesized via the melt-quenching method as described in Ref.(15). The chemical compositions of the glasses were analyzed by energy dispersive X-ray spectrometer (EDX) using commercial $Ge_{33}As_{12}Se_{55}$ glass (Amorphous Material Co.) as a reference. The measurements were performed at different positions of the glass and the averaged results were used as the final composition. It was found that, the difference between the nominal and final composition was less than 0.5%. A conventional X-ray diffractometer was used to examine if the glass contains any crystalline structure. A differential scanning calorimetry (DCS, TA-Q series) was used to measure T_g and a Vickers micro-indenter (Everone MH-3, Everone Enterprises Ltd., Shanghai, China) was used to measure the Vickers-hardness of the glasses. The density, ρ, of the samples was measured using a balance (Mettler-Toledo Ltd., Switzerland) with a MgO crystal used as a reference.

The transmission spectra of the glasses were recorded utilizing a spectrometer (Lambda 950, PerkinElmer) in visible and near infrared region and a Fourier transform infrared spectrometer (Nicolet 380, Thermo Scientific) in a spectral range between 2.5 and 25 μm. The linear refractive index was measured in a wavelength range between 1.7-20 μm by using a variable angle spectroscopic ellipsometer (IR-VASE, J. A. Woollam, Lincoln, NE). To determine optical bandgap E_g, the glasses were grinded into fine powers before they were placed onto sapphire wafer. Then they were heated to a temperature 50-100 ^oC above T_g , and pressed with a polished vitreous carbon plate in a nitrogen atmosphere. E_g was finally extracted from the Tauc plots of the absorption spectra of the hot-pressed 10-30 μm thick films.

A Ti: sapphire laser (Orpheus-HP, Light Conversion, USA) with 170 fs pulse duration at 1 kHz repetition rate was used to excite optical nonlinearity via the Z-scan method. During the measurements, the laser was split into two light beams, one of them was monitored by an energy detector (S470C, Thorlabs, USA) as a reference, and another one as the pump light was detected by a sensitive pyroelectric power probe (S180C, Thorlabs, USA), and focused into Gaussian beam by a 30 cm focal length.

To measure laser damage, a Ti:sapphire laser (Coherent, Mira 900D) emitting 150 fs pulses with a wavelength of ~800 nm ($\hbar_\omega$ = 1.6 eV) and a repetition rate of 1 kHz was introduced into the polished glass surface to examine if the surface was damaged by 1000 light pulses in air. The beam with linear polarization was focused onto glass surface by a×5 achromatic objective lens. An optical attenuation device consisting of a half-wave plate and a polarizer that can tune the power and polarization was placed between the laser and the glass. The damage induced by laser beam were in situ examined by a camera. The size of damaged spots was further examined by an optical microscope (Keyence, JAPAN, VEX-1000E) and an atomic force microscope AFM (Cypher-HV).

3. Results and Discussion

Figure 1 shows the transmission spectra of $Ge_xGa_4S_{96-x}$ glasses. It is found that, the transmission edge at shorter wavelength range shifts to longer wavelength, while that at longer wavelength range shrinks to the shorter wavelength with increasing Ge content in the glass. All the glasses exhibit good transparency with more than 60% transmission from 0.75 to 10 μm.

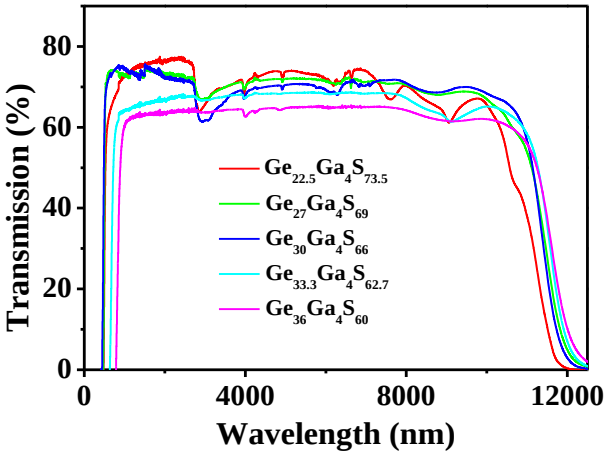

Fig. 1. Transmission spectra of the glasses.

Figure 2 shows typical Z-scan curve of $Ge_{30}Ga_4S_{60}$ glass in the closed aperture. With the increase of the scanning distance Z, Z-scan profile exhibit pre-focal peak first, and then a post-focal valley. We also observed the similar S-scan curves in other glasses. Since the lifetime of the free carrier absorption (FCA) in chalcogenide glasses is in a time scale of nanoseconds[16], which is much longer than 170 fs pulse width used in the measurements, here we neglected the effect of FCA on the measurements. We also ignored thermal effect in the experiments since only 400 μW average power from the laser was used in the experiments.

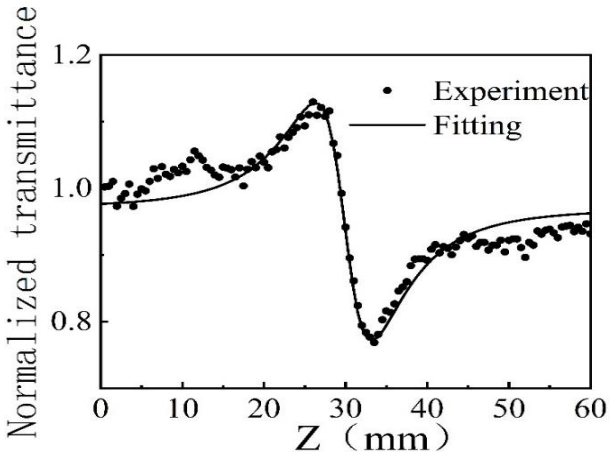

Fig. 2. Typical closed-aperture Z-scan curve and its fitting for Ge30Ga4S60 at 1550 μm.

Figure 3 (a) is density and linear refractive index (n_0) versus Ge content in $Ge_xGa_4S_{96-x}$ glasses. It can be seen that, both density and n_0 increase with increasing content of Ge in glasses. Since Ge has larger atomic mass and more polarizable electronic clouds [17], the replacement of S by Ge in $Ge_xGa_4S_{96-x}$ glasses leads to the increase of the density and n_0. Figure 3(b) show the

dependence of nonlinear index n_2 and two-photon absorption coefficient β on Ge content. It was found that, unlike those in Fig.3(a), n_2 decreases from 0.65×10^{-14} cm^2/W in the glass with Ge content of 22.5 to 0.46×10^{-14} cm^2/W in that with Ge content of 30%, and then increase to 1.19×10^{-14} cm^2/W in that with Ge content from 36%. On the other hand, two-photon absorption coefficient gradually increases from 0.06 to 0.35. The evolution of the nonlinear index n_2 and two-photon absorption coefficient β on Ge content in $Ge_xGa_4S_{96-x}$ is similar to those observation in Ref.(18). These linear and nonlinear parameters, together with T_g, density, hardness, and E_g of the glasses are listed in Table 1.

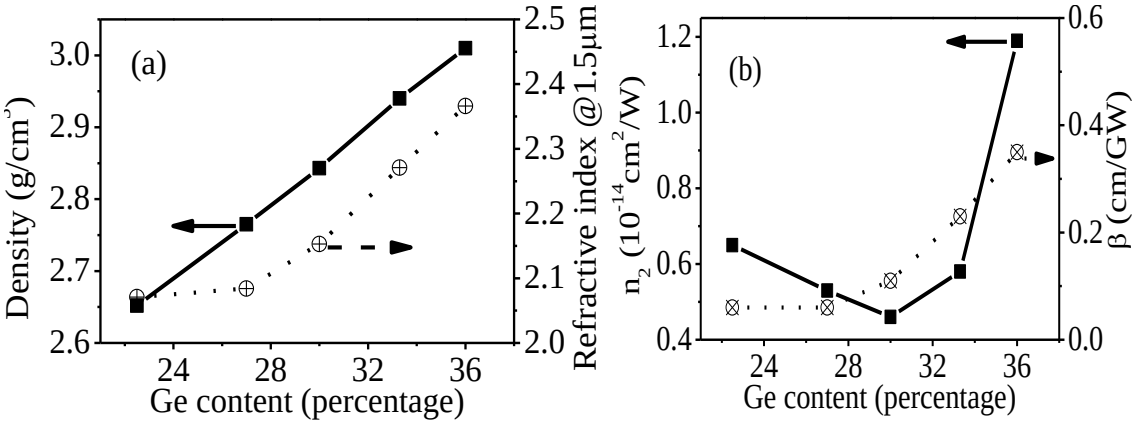

Fig. 3. Density and linear refractive index $\boldsymbol{n_0}$*, (a) and the third-order nonlinear refractive index* $\boldsymbol{n_2}$ *and two-photo absorption coefficient β (b) versus Ge content. The lines in figure are guided to the eyes.*

The semi-empirical Miller's rule gives the relationship between the linear and nonlinear susceptibility χ^3 as following [19],

$$\chi^3 = \frac{n_2 n_0^2}{0.0395} = \alpha\left[\frac{(n_0^2-1)}{4\pi}\right]^4 \quad (1)$$

where χ^3 is the third order susceptibility in esu; α is the Miller's coefficient for chalcogenide glass. Figure 4(a) shows the relationship between χ^3 and $[(n_0^2-1)/4\pi]^4$, where the solid symbols are the experimental data and the line is the fitting based on Eq. (1) using a value of 7.5×10^{-11} for α. Figure 4(b) shows the relation between n_0 and n_2, where the solid line is the transform of Eq. (1),

$$n_2 = 1.18\times10^{-16}\frac{(n_0^2-1)^4}{n_0^2}cm^2 \quad (2)$$

Some points diverge from the curves in Fig.s 4(a) and (b) is due to the errors in Z-scan measurements. The difference between the experimental and fitting results is comparable or even less than the uncertainties in most experiments. The value of α and the coefficient in Eq.(2) obtained in the present measurements are in good agreement with those for chalcogenide glasses [20,21]. This confirms that the relation between n_0 and n_2 in $Ge_xGa_4S_{96-x}$ glasses can be well described by the Miller's rule.

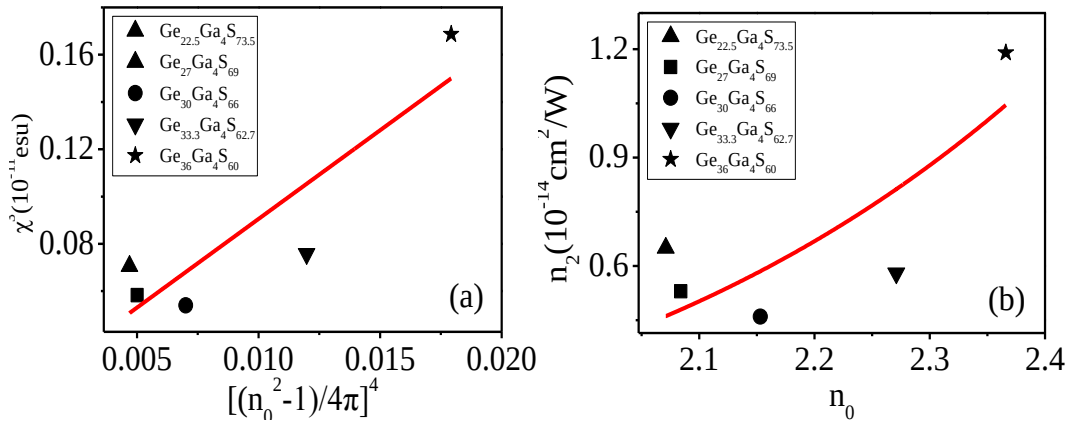

Fig. 4. (a) The nonlinear susceptibility and $(n_0^2 - 1)/4\pi$. The line is the fitting based on Eq. (1). (b) n_2 versus n_0 , the line is the fitting based on Eq. (2).

On the other hand, the present results regarding the values of n_2 are one or two order of magnitude less than those in Se- and Te-based chalcogenide glasses [20, 21], but are in agreement with those in Ref.s [12-14]. Although n_2 becomes larger with increasing Ge content and the maximum n_2 can be achieved in $Ge_{36}Ga_4S_{60}$ glass, the two-photon absorption coefficient reaches maximum as well.

For laser damage, the minimum value of the energy density that induces observable damages in the glass is defined as the damage threshold. During the experiments, the diameter of the damaged spot D was measured at different radiate fluence F. The radiate fluence F at the center of Gaussian beam is given by [22],

$$F = \frac{2E_{pulse}}{\pi w_0^2} = \frac{2P_{avg}}{R\pi w_0^2} \tag{3}$$

where w_0 is the beam waist radius of Gaussian-type beam, E_{pulse} is the total pulse energy, P_{avg} is the averaged power, and R is the repetition rate of the laser pulse. The ablation threshold fluence F_{th} is thus obtained from the relation [22]

$$D^2 = 2w_0^2(lnF - ln\,F_{th}) \tag{4}$$

Fig. 5(a) shows surface morphology of typical damages in $Ge_{30}Ga_4S_{66}$ glass. Damage profile might vary in different spots because of the random distribution of the sputtered dusts on the surfaces and unstable laser power, etc. The corresponding AFM image in Fig.5(b) shows a crater-like morphology with the burrs in the rim of the crater. Such a morphology is not related to the polarization of the laser light. To avoid any errors of F_{th} in the experiments, the measurements were performed at more than 5 different positions, and the average value of F_{th} was listed in Table 1 for each glass. The margin of error for the damage threshold was within ±10 %.

Table 1. T_g, density, E_g, refractive index (n_0), nonlinear refractive index (n_2), two photon absorption coefficient β, figure of merit (FOM), hardness and laser damage threshold in $Ge_xGa_4S_{96-x}$ glasses.

Composition (in mol.%)	***T_g*(°C)**	***Density* (g/cm^3)**	***E_g* (±0.01eV)**	***n_0* (±0.001)**	***n_2*(10^{-14} cm^2/W) ±15%**	***β*(cm/GW) ±15%**	***FOM* (n2/βλ)**	***Hardness* (kg/cm^2)**	***Damage Threshold* (mJ/cm^2)**
$Ge_{22.5}Ga_4S_{73.5}$	285.6	2.652	2.45	2.071	0.65	0.06	6.99	191	298
$Ge_{27}Ga_4S_{69}$	347.6	2.765	2.58	2.084	0.53	0.06	5.70	207	321
$Ge_{30}Ga_4S_{66}$	434.7	2.843	2.69	2.153	0.46	0.11	2.70	220	345
$Ge_{33.3}Ga_4S_{62.7}$	359.3	2.94	2.11	2.271	0.58	0.23	1.72	208	323
$Ge_{36}Ga_4S_{60}$	336.2	3.01	1.86	2.366	1.19	0.35	2.19	198	311

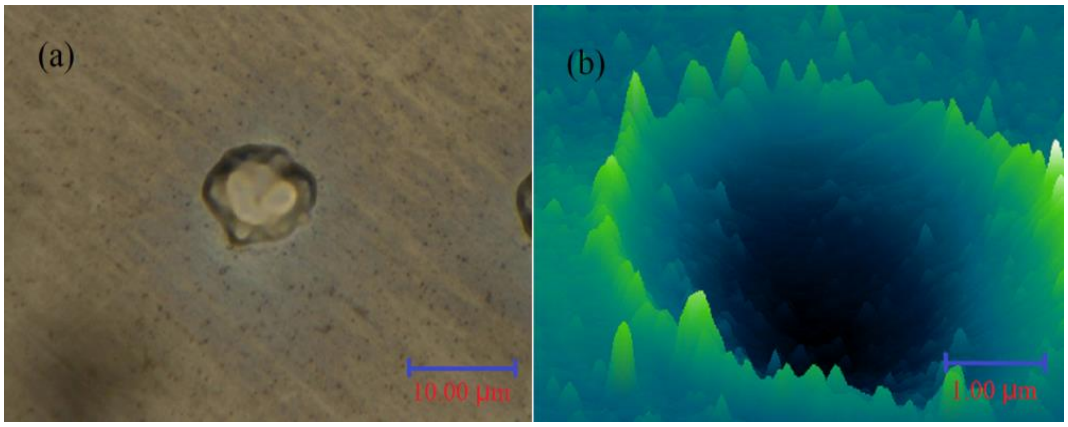

Fig. 5. Surface morphology of damaged $Ge_{30}Ga_4S_{66}$ glass by optical microscope (a) and AFM (b)

Going back to the various physical parameters in Table 1, we found that, both T_g, E_g, Hardness and laser damage threshold increase before they reach a maximum in $Ge_{30}Ga_4S_{66}$ glass which corresponds to chemically stoichiometric composition $(GeS_2)_{90}(Ga_2S_3)_{10}$, and then decrease with increasing Ge content, exhibiting a threshold maximum in $Ge_{30}Ga_4S_{66}$ as shown in Fig.6. The maximum value of T_g in $Ge_{30}Ga_4S_{66}$ indicates that the stoichiometric glass has the best network connectivity [23]. Mahadevan et al. investigated the compositional dependence of T_g in Ge-Sb-Se glasses [24], and found that the maximum value of T_g appears in the glass with stoichiometric composition. Such an evolution of T_g suggested that, Ge-Sb-Se glass network consists of demixed blocks of $GeSe_{4/2}$ and $SbSe_{3/2}$ [25,26], where phase separation in the nano-or micro-meter scale can occur above the threshold. Similarly, demixed structural units could be $GeS_{4/2}$ and $GaS_{3/2}$, where these threshold behaviors of physical properties in GeGaS glasses can be traced to "demixing" of networks above the chemical thresholds. This has been demonstrated by structural investigations of GeGaS glasses via analyzing their Raman and X-ray photoelectron spectra [15,27]. Obviously, excellent network connectivity implies less homopolar bonds, and thus large amount of heteropolar bonds with strong chemical bonding energy in the glass, leading to a maximum value of hardness and laser damage threshold.

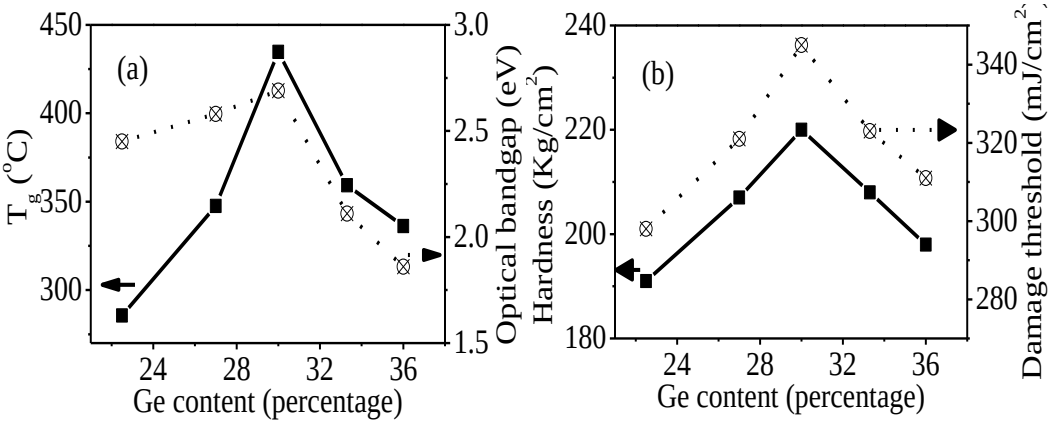

Fig. 6. T_g and E_g (a), and hardness and laser damage threshold (b) as a function of Ge content.

In terms of the practical applications in photonic devices, the present results indicate that, although large optical nonlinearity can be achieved in $Ge_{36}Ga_4S_{60}$ glass, the two-photon absorption coefficient also increases. Considering the value of FOM, it could be a better option to use the glass with chemically stoichiometric composition, where its relatively low optical nonlinearity can

be compensated by a high laser damage threshold, e.g., optical devices can be pumped by a high laser power. This is in sharp contrast with the resutls in the previous literatures where only glasses containing less than 15% Ge were used for rare earth doping[6,8].

4. Conclusion

$Ge_xGa_4S_{96-x}$ glasses with x from 22.5 to 36 were prepared and their physical properties were measured in this paper. The results indicated that, while both T_g, E_g, hardness and laser damage have a threshold behaviour exhibiting a maximum in the $Ge_{30}Ga_4S_{66}$ glass, linear refractive index increases with increasing Ge content, nonlinear refractive index has a minimum in $Ge_{30}Ga_4S_{66}$, and their correlation can be well described by the Miller's rule. To screen the best glass as a host RELs doping for the applications in optical amplifier, the glass with chemically stoichiometric composition appears to be the best since it has reasonable optical nonlinearity and two photon absorption, high FOM and high laser damage threshold.

Acknowledgements

The authors would like to thank to the National Key R&D Program of China (2020YFB1805900); Natural Science Foundation of China (Grant No. 61775109); 3315 Innovation Team in Ningbo City, Zhejiang Province, China; K.C. Wong Magna Fund in Ningbo University, China.

References

[1] K. Tanaka and K. Shimakawa, Amorphous Chalcogenide Semiconductors and Related Materials, Springer, 2011; https://doi.org/10.1007/978-1-4419-9510-0

[2] R. P. Wang, Amorphous chalcogenides: advances and applications, Pan Stanford Publishing, 2014; https://doi.org/10.1201/b15599

[3] Zakery and S. R. Elliott, Optical Nonlinearities in Chalcogenide Glasses and their Applications, Springer, 2007.

[4] P. Ma, D. Y. Choi, Y. Yu, X. Gai, Z. Y. Yang, S. Debbarma, S. Madden and B. Luther-Davies, Low-loss chalcogenide waveguides for chemical sensing in the mid-infrared, Optics Express 21 (24), (2013) 29927-29937; https://doi.org/10.1364/OE.21.029927

[5] P. Ma, D. Y. Choi, Y. Yu, Z. Y. Yang, K. Vu, T. Nguyen, A. Mitchell, B. Luther-Davies and S. Madden, High Q factor chalcogenide ring resonators for cavity-enhanced MIR spectroscopic sensing, Optics Express 23 (15), (2015) 19969-19979; https://doi.org/10.1364/OE.23.019969

[6] Angela B Seddon, Z. Q. Tang, David Furniss, Slawomir Sujecki and Trevor M Benson, Progress in rare-earth-doped mid-infrared fiber lasers, Optical Express 18(5),(2010)26704—26719; https://doi.org/10.1364/OE.18.026704

[7] R. P. Wang, K. L. Yan, M. J. Zhang, X. Shen, S. X. Dai, X. Y. Yang, Z. Y. Yang, Anping Yang, Bin Zhang, Barry Luther-Davies, Chemical environment of rare earth ions in $Ge_{28.125}Ga_{6.25}S_{65.625}$ glass-ceramics doped with Dy^{3+}, Applied Physics Letters 107 (2015) 161901; https://doi.org/10.1063/1.4934261

[8] J.S. Sanghera, I.D. Aggarwal, Active and passive chalcogenide glass optical fibers for IR applications: a review, J. Non-Cryst. Solids 256&257 (1999) 6-16; https://doi.org/10.1016/S0022-3093(99)00484-6

[9] Y. Yu, B. Zhang, X. Gai, C. Zhai, S. Qi, W. Guo, Z. Yang, R. Wang, D. Y. Choi, S. Madden and B. Luther Davies, 1.8-10 μm mid-infrared supercontinuum generated in a step-index chalcogenide fiber using low peak pump power, Opt. Lett. 40 (6) (2015) 1081-1084;

https://doi.org/10.1364/OL.40.001081
[10] Y. Yu, X. Gai, P. Ma, D.-Y. Choi, Z. Yang, R. Wang, S. Debbarma, S. J. Madden and B. Luther-Davies, A broadband, quasi-continuous, mid-infrared supercontinuum generated in a chalcogenide glass waveguide, Laser &Photonics Rev. 8 (5) (2014) 792-798; https://doi.org/10.1002/lpor.201400034
[11] Z. M. Zhao, B. Wu, X. S.Wang, Z. G. Pan, Z. J. Liu, P. Q. Zhang, X. Shen, Q. H. Nie, S. X. Dai, and R. P. Wang, Mid-infrared supercontinuum covering 2.0-16 μm in a low-loss telluride single-mode fiber, Laser & Photonics Rev. 11 (2) (2017) 792-798; https://doi.org/10.1002/lpor.201700005
[12] G. P. Dong, H. Z. Tao, X. D Xiao, C. G. Lin, Y. Q. Gong, and X. J. Zhao, Study on the third and second-order nonlinear optical properties of GeS_2-Ga_2S_3-AgCl chalcohalide glasses, Optics Express 15(5), 2398-2408(2007); https://doi.org/10.1364/OE.15.002398
[13] H. T. Guo, H. Y. Chen, C. Q. Hou, A. X. Lin, Y. G. Zhu, S. D. Lu, S. X. Gu, M. L, B. Peng The third-order optical nonlinearities of Ge-Ga-Sb(In)-S chalcogenide glasses, Material research bulletin 46, 756-770(2011); https://doi.org/10.1016/j.materresbull.2010.11.020
[14] X. Y. Zhang,, F. F. Chen, R. Q. Lin, Y. C. Huang, S. X. Dai, Q. H. Nie, X. H. Zhang, W. J, Investigation of third-order optical nonlinearities of copper doped germanium-gallium-sulfur chalcogenide glasses, JNCS 475,167-171(2017); https://doi.org/10.1016/j.jnoncrysol.2017.09.002
[15] X. Y. Yang, M. J. Zhang, K. L. Yan, L. Y. Han, Q. Xu, H. T. Liu, R. P. Wang, Controllable formation of the crystalline phases in Ge-Ga-S chalcogenide glass-ceramics, Journal of American Ceramic Society 100,74-80(2017); https://doi.org/10.1111/jace.14492
[16] B. Gu, J. Wang, J. Chen, Y. X. Fan, J. P. Ding, and H. T. Wang, Z-scan theory for material with two- and three-photon absorption, Opt. Express 13(23), 9230-9234 (2005); https://doi.org/10.1364/OPEX.13.009230
[17] Asobe. M, Kanamori. T, Kubodera K. I. Application of highly nonlinear chalcogenide glass fibers in ultrafast all-optical switches, IEEE Journal of Quantum Electronics, 1993, 29(8): 2325-2333; https://doi.org/10.1109/3.245562
[18] A. Prasad, C. J. Zha, R.P. Wang, A. Smith, S. Madden, B. Luther-Davies, Properties of $Ge_xAs_ySe_{1-x-y}$ glasses for all-optical signal processing, Optics Express 16 (4) (2008) 2804-2815; https://doi.org/10.1364/OE.16.002804
[19] R. W. Boyd, Nonlinear Optics, second Edition, Academic Press Inc. 2003.
[20] T. Wang, X. Gai, W. Wei, R. P. Wang, Z. Yang, X. Shen, S. Madden and B. Luther-Davies, Systematic z-scan measurements of the third order nonlinearity of chalcogenide glasses, Opt. Mater. Express 4 (5) (2014) 1011-1022; https://doi.org/10.1364/OME.4.001011
[21] Q. Li, R. P. Wang, F. U. Xu, X. Wang, and X. Gai, Third-order nonlinear optical properties of Ge-As-Te chalcogenide glasses in mid-infrared, Optical Materials Express 10 (6) (2020) 1413-1420; https://doi.org/10.1364/OME.392655
[22] M. Xie, S. Dai, C. You, P. Zhang, C. Yang, W. Wei, G. Li, and R. Wang, J. Phys. Chem. C, 122, 1681 (2018); https://doi.org/10.1021/acs.jpcc.7b10894
[23] M. Micoulaut and G. G. Naumis, Glass transition temperature variation, cross-linking and structure in network glasses: A stochastic approach. Europhys Lett 1999, 47, 568-574; https://doi.org/10.1209/epl/i1999-00427-7
[24] S. Mahadevan and A. Giridhar; Floppy to Rigid Transition and Chemical Ordering in Ge-Sb(as)-Se Glasses. J Non-Cryst Solids 1992, 143, 52-58; https://doi.org/10.1016/S0022-3093(05)80552-6
[25] S. Bhosle, K. Gunasekera, P. Boolchand and M. Micoulaut, Melt Homogenization and Self-Organization in Chalcogenides-Part II. Int. J. Appl. Glass Sci. 2012, 3, 205-220; https://doi.org/10.1111/j.2041-1294.2012.00092.x
[26] W.H. Wei, R.P. Wang, X. Shen, L. Fang, Barry Luther-Davies, Correlation between structure and physical properties in Ge-Sb-Se glasses, J. Physical Chemistry C 117,16571-16576(2013); https://doi.org/10.1021/jp404001h

[27] Q. Xu, X. Yang, M. Zhang, and R. P. Wang, The ability of $Ge_xGa_4S_{96-x}$ chalcogenide glasses dissolving rare earth probed by x-ray photoelectron spectra analysis, Materials Research Express 6(8),085212(2019); https://doi.org/10.1088/2053-1591/ab23be